RSC Advances

PAPER

View Article Online
View Journal | View Issue

Cite this: *RSC Adv.*, 2025, **15**, 22460

Facile calixarene-based sensor array strategy for quality evaluation of Yinxing Mihuan oral solution†

Kejing Niu,‡[a] Mengyu Ye,‡[a] Yun Lyu,[a] Wenqian Cheng,[a] Shaoqing He,[d] Dan Liu*[c] and Huijuan Yu*[ab]

Received 10th June 2025
Accepted 20th June 2025

DOI: 10.1039/d5ra04079e

rsc.li/rsc-advances

To facilitate efficient and rapid quality evaluation of traditional Chinese medicine (TCM) preparations, we introduced an innovative macrocycle-based fluorescence sensing strategy. Herein, an array of calixarene-based sensors was designed to assess the batch-to-batch consistency and precise feeding of raw materials of Yinxing Mihuan oral solution (YMOS), which is used to treat cardiovascular and cerebrovascular diseases in the clinic, highlighting the feasibility of the established supramolecular fluorescence sensing method. Using indicator displacement assay (IDA), the molecular recognition between calixarenes and the tested compounds from YMOS was converted into multi-fluorescence signals by extruding the indicators from their respective hosts, whose mechanisms were unveiled by theoretical calculations. By employing the constructed three-element sensor array, a standard fluorescent fingerprint was displayed by "spider-web" mode to evaluate the quality consistency of the YMOS samples. Moreover, the optimized QAC5A·EY reporter pair was successfully applied to guarantee precise feeding of raw materials during the manufacturing process of YMOS. The calixarene-based sensor array method offers a comprehensive evaluation for YMOS in a facile and high-throughput style, conducive to improving quality evaluation of TCM.

Introduction

As a primary modality in the clinical application of traditional Chinese medicine (TCM), TCM compound preparations are composed of multiple herbs and characterized by complex compositions,[1] which are of great significance in the prevention and treatment of diseases, as well as in rehabilitation and health care. Admittedly, the quality consistency evaluation of TCM compound preparations is essential to ensure the security and validity of their clinical applications.[2] In recent years, significant advancements have been achieved in research on chemical substances and the quality control of TCM compound preparations. Technical methods for appraising the quality consistency of TCM compound preparations encompass chromatography, spectroscopy, and bioassay methods.[3] The extensively used chromatographic techniques, which rely on chemical components separation for fingerprint analysis and quantification of quality markers, are hindered by the unavailable reference standards, high reagent consumption, and insufficient throughput to meet inspection requirements.[4] Therefore, it is imperative to explore new technologies and methods for consistency evaluation.

Yinxing Mihuan oral solution (YMOS) is a widely used TCM compound preparation comprising *Ginkgo biloba* extract and *Armillaria mellea* powder, predominantly employed in the treatment of cardiovascular and cerebrovascular diseases.[5] The current Chinese Pharmacopoeia (2020 edition) specifies the total content of flavonol glycosides from GBE.[6] It was reported that liquid chromatography-based methods were employed to develop multi-components quantification for YMOS,[7–9] including flavones, nucleosides, organic acids, monosaccharides, polysaccharides, and additives, which laid the foundation for the quality control and evaluation of YMOS. As a popular method, spectroscopic techniques, such as near-infrared spectroscopy, Fourier transform infrared spectroscopy, and fluorescence spectroscopy, have been used in assessing the quality consistency of compound Yuxingcao mixture,[10] Belamcandae rhizoma antiviral injection,[11] and Qufeng Zhitong capsule[12] by taking simple sample preparation, high throughput, and environmental friendliness into account. Therefore, spectroscopic techniques can effectively

[a]*State Key Laboratory of Chinese Medicine ModernizationTianjin University of Traditional Chinese Medicine, Tianjin, 301617, China. E-mail: huijuanyu@tjutcm.edu.cn*

[b]*Haihe Laboratory of Modern Chinese Medicine, Tianjin, 301617, China*

[c]*Department of Pharmacy, 967th Hospital of the Joint Logistics Support Force of the Chinese People's Liberation Army, Dalian, Liaoning, 116011, China. E-mail: dlld3836@163.com*

[d]*Xi'an Buchang TCM Cardiovascular and Cerebrovascular Hospital, Xi'an, Shaanxi, 710082, China*

† Electronic supplementary information (ESI) available: Screening of sensing units, structures of the analytes, fluorescence spectra of titration, additional theoretical calculation figures, additional tables. See DOI: https://doi.org/10.1039/d5ra04079e

‡ Kejing Niu and Mengyu Ye contributed equally to this work.

evaluate the quality consistency of TCM compound preparations.

Supramolecular fluorescence sensing technology, emerging as a powerful tool in the field of TCM due to its easy operation, high sensitivity, and high throughput capabilities,[13] has been widely utilized for screening bioactive compounds in TCM,[14,15] assessing the quality of TCM,[12] and detecting the potential aflatoxins in TCM.[16] By employing the indicator displacement assay (IDA), the analyte competes with the dye for the cavity of the macrocyclic host, displacing the dye and resulting in a change in the fluorescence intensity of the system.[13] Conventional single sensing is designed based on the "lock and key" principle, optimizing a host–guest reporter pair for detecting target analyte, which necessitates extremely high specificity and sensitivity for the sensing system.[17] However, single sensing systems can not detect analytes with diversified structures, especially when analyzing complex mixtures, such as TCM preparations. Sensor arrays are capable of differentiating subtle changes resulted from multiple target analytes in complex systems.[18] In a sensor array, multiple sensor elements are essential units that selectively interact with corresponding target analytes, generating unique "fluorescent fingerprints" based on multi-fluorescent responses, thereby enabling the quality consistency evaluation of TCM preparations.[18,19] The library of macrocyclic hosts provides broad-spectrum recognition capability for sensing different compounds. It is exciting that supramolecular-based fluorescence sensor arrays have shown remarkable capability in discrimination of nucleotides,[20] glycosaminoglycans,[21] honey,[22] as well as for assessing the quality of TCM compound preparations, such as Qufeng Zhitong capsule.[12] To the best of our understanding, no prior efforts have been made to develop a supramolecular fluorescence sensor array specifically designed for quality evaluation of YMOS.

In this study, we specifically selected the host·guest reporter pairs as sensing elements to successfully construct a highly efficient calixarene-based sensor array (Scheme 1). The sensor array, which comprises three macrocyclic receptors, engages with the analytes through host·guest complexation, generating distinctive fluorescent responses for YMOS sample by IDA strategy. A "spider-web" mode was utilized to assess the fluorescent fingerprint of YMOS samples, facilitating systematic analysis of batch-to-batch consistency of quality. Furthermore, the selective recognition mechanism between the calixarene and the tested compounds of YMOS was elucidated through the determination of association constants and supported by theoretical calculations. The QAC5A·EY sensing element has been successfully employed to differentiate the self-made YMOS samples with various combinations of *Ginkgo biloba* extract and *Armillaria mellea* powder. Our simple and high-throughput method, which utilizes a supramolecular fluorescence sensing detection, greatly enhances the efficiency of large-scale applications on quality evaluation of TCM.

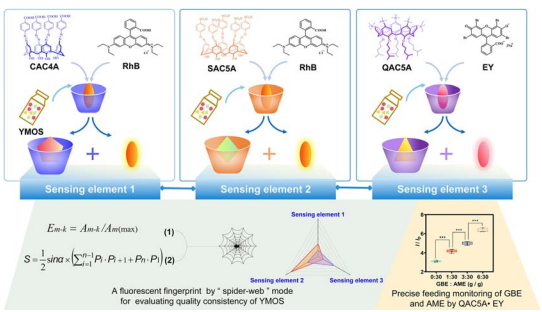

Scheme 1 Schematic diagram of supramolecular sensor array based on IDA.

Experimental

Reagents and materials

Twelve batches of YMOS numbered as YM1–YM12, *Ginkgo biloba* extract (GBE), and *Armillaria mellea* extract (AME) were provided by Qionglai Tianyin Pharmaceutical Co., Ltd. (Sichuan, China). *p*-Sulfonatocalix[4]arenes (SC4A), *p*-sulfonatocalix[5]arenes (SC5A), *p*-sulfonatocalix[6]arenes (SC6A), sulfonated azocalix[5]arene (SAC5A), carboxylazocalix[4]arene (CAC4A), and 5,11,17,23,29-penta(trimethylammonium)-31,32,33,34,35-penta(4-methylpentyloxy)calix[5]arene (QAC5A) were provided by Dongsheng Guo's research group from the College of Chemistry, Nankai University.[21,23–27] Rhodamine B (RhB), eosin Y (EY), *trans*-4-[4-(dimethydamino)styryl]-1-methylpyridinium iodide (DSMI), lucigenin (LCG), 2-(*p*-toluidinyl)naphthalene-6-sulfonic acid (2,6-TNS), dapoxyl, 4′,6-diamindino-2-phenylin-dole (DAPI), β-cyclodextrin (β-CD), cucurbit[6]uril (CB[6]), cucurbit[7]uril (CB[7]), sodium hydroxide, and methanol (HPLC grade) were purchased from Sigma-Aldrich Co., Ltd. (St. Louis, Missouri, USA). Methylene blue (MB) was purchased from Merck KGaA Co., Ltd. (Darmstadt, Germany). Oxazine 1 (OX1) was purchased from AmyJet Scientific Inc. (Wuhan, China). Sodium benzoate (SoB), protocatechuic acid (Pra), rutin (QGR), ginkgolides A (GinA), uridine (Uri), and tween 80 (HPLC grade) were purchased from Shanghai Yuanye Biotechnology Co. Ltd. (Shanghai, China). Water was purified using a Milli-Q water purification system (Millipore, Billerica, MA, USA). *N*-(2-Hydroxyethyl)piperazine-*N*′-2-ethanesulfonic acid (HEPES) buffer (10 mM, pH 7.4) solution was prepared by ultrapure water.[28] D_2O and 3-(trimethylsilyl) propionic-(2,2,3,3-d_4) acid sodium salt (TSP-d_4) were purchased from Cambridge Isotope Laboratories, Inc. (USA).

Instruments

Equipped with a Varian Cary single-cell peltier accessory for temperature control, a Varian Cary Eclipse spectrometer (Agilent Technologies Inc., USA) was performed to record steady-state fluorescence spectra in a conventional quartz cell (light path of 10 mm). DL-720B ultrasonic cleaning machine was obtained from Shanghai Zhixin Instrument Co., Ltd. (Shanghai, China). Laboratory pH meter FE20 was purchased from Mettler Toledo International Co., Ltd. (Switzerland). DK-98-II electric-heated thermostatic water bath was procured from Tianjin

Teste Instrument Co., Ltd. (Tianjin, China). AVANCE III 500 MHz spectrometer was obtained from Bruker (Fällanden, Switzerland).

Preparation of self-made YMOS sample

In accordance with the reported method,[29] the self-made YMOS sample with different combination of GBE and AME were prepared as follows. Different weights of GBE (0, 0.05, 0.15, 0.30 g) were gradually added to Tween 80 (0.25 g), which had been dissolved in 10 mL ultrapure water, with continuous stirring at 80 °C water bath until it completely dissolved. Then, AME (1.5 g) was diluted with ultrapure water and stirred in a 70 °C water bath for 30 min, followed by filtration. After allowing the above solutions to cool down to room temperature, they were transferred into 50 mL volumetric flask and diluted to scale with ultrapure water. Subsequently, sample solutions of self-made YMOS with different combinations of GBE and AME (0 : 30, 1 : 30, 3 : 30, and 6 : 30; g g^{-1}) were prepared in parallel for three replicates.

Fluorescence spectroscopy

The steady-state fluorescence spectra were recorded using a Varian Cary Eclipse spectrometer (Agilent Technologies Inc., USA) fitted with a Varian Cary single-cell peltier accessory. The titration experiments were conducted in a standard 10 × 10 × 45 mm^3 quartz cell with a 10 mm optical path length. The fluorescence spectra of CAC4A·RhB, SAC5A·RhB, and QAC5A·EY reporter pairs were recorded at the respective excitation wavelengths of dyes (Rhb at 554 nm and EY at 517 nm) in HEPES buffer solution (10 mM, pH 7.4) at 25 °C.

Methodological evaluation

In HEPES buffer solution (10 mM, pH 7.4), the fluorescent intensity of the host·dye reporter pairs (CAC4A·RhB, SAC5A·RhB, and QAC5A·EY) at the respective emission wavelengths of 576 nm (RhB) and 537 nm (EY) was recorded before (I_0) and after (I) adding 5 μL YMOS sample solution at 25 °C, respectively. The intra-day precision of each sensing element was analyzed by calculating the relative standard deviation (RSD) value of the six I/I_0 data for the same YMOS sample solution. The inter-day precision of each sensing element was carried out by calculating the RSD value of the I/I_0 data obtained from consecutive three-days measurements of sample solutions prepared by the same batch of YMOS. The repeatability test was assessed by calculating the RSD value of the I/I_0 values determined by each sensing element for six sample solutions from one batch of YMOS. The stability experiment was evaluated by calculating the RSD value of I/I_0 values determined by each sensing element for the same YMOS sample solution at 0, 2, 4, 6, 8, and 10 h, respectively.

Association constant measurement

Direct fluorescence titrations of dye with host were carried out by gradually adding the host solution to the HEPES buffer solution containing appropriate concentration of dye. The association constant (K_a/M^{-1}) of host and dye was obtained by fitting the fluorescence intensity of dye at its maximum emission wavelength to the concentration of tested host. Competitive fluorescence titrations were undertaken by gradually adding the tested compound solution to the HEPES buffer solution containing appropriate concentration of host·dye complex, which generated variation in the fluorescence intensities of the dye. The K_a of hosts with the tested compounds (SoB, Pra, QGR, GinA, and Uri) was obtained by fitting the fluorescence intensity of dye at its maximum emission wavelength (RhB at 576 nm and EY at 537 nm) to the concentration of tested compounds. By the Origin software, fitting anlysis was performed to respectively obtain the K_a values of the host·dye complex and the host·tested compound complex using a 1 : 1 binding model (oneHost_oneGuest) and a 1 : 1 competitive binding model (oneHost_oneGuest_oneCompetitor) in a non-linear manner. The fitting modules were comprehensively described and introduced in our published work.[30] Throughout the titrations, the concentrations of the dye and host·dye complex were kept to be constant in direct fluorescence titration and competitive fluorescence titration experiments, respectively. All experiments were carried out in HEPES buffer solution (10 mM, pH 7.4) at 25 °C. Data were displayed as mean ± standard deviation (SD) ($n = 3$).

Theoretical calculations

Using Gaussian 16 program[31] and the solvation model based on density (SMD),[32] all density functional theory (DFT) calculations were implemented for the host with the tested compound (analyte). The host·analyte complex of geometric optimization was carried out at the B3LYP/6-31G(d)[33] level of theory, incorporating Grimme's D3 dispersion correction.[34] The default convergence criteria of Gaussian 16 were utilized for molecular geometry optimization. The energies of the host·analyte complex (E_{HA}), the host (E_H) and the analyte (E_A) were obtained from the Gaussian 16 output files. The binding energy of the host·analyte complex was calculated as $\Delta E = E_{HA} - (E_H + E_A)$. Performed by the Multiwfn 3.8 software, the molecular electrostatic potential (MEP) analysis and independent gradient model based on Hirshfeld partition (IGMH) analysis of host·analyte complex were accomplished.[35] The calculation results was displayed by visual molecular dynamics (VMD) software.[36]

NMR spectroscopy

^{1}H NMR spectra were recorded on an AVANCE III 500 MHz spectrometer (Bruker, Fällanden, Switzerland) using TSP-d_4 as an internal reference at 298 K. Samples of SAC5A·GinA, SAC5A, and GinA for ^{1}H NMR measurement were prepared in D_2O.

Results and discussion

Construction and methodological investigation of supramolecular fluorescence sensor array for evaluating the quality of YMOS sample

The selection and combination of sensing elements are pivotal in constructing a supramolecular fluorescence sensing array.[18] Typically, a sensing element in such arrays consists of a macrocyclic receptor and a fluorescent indicator (dye), which

are linked through non-covalent interactions such as hydrogen bonding, electrostatic interactions, and hydrophobic interaction.[37] Based on IDA, the introduced target analyte can compete with the dye for the macrocyclic receptor's cavity, leading to an enhanced (switch-on) or quenched (switch-off) fluorescence signal of the sensing system.[38]

For successful detection of YMOS samples *via* IDA strategy, the crucial challenge is to identify a host·guest reporter pair that can generate a substantial fluorescence signal response in the presence of the YMOS sample solution. Classical macrocycles, such as cyclodextrin (CD),[39] calixarene (CA),[40] and cucurbituril (CB),[41] possess unique structural features, which confer their distinct superior recognition properties. In this study, we investigated the classical host·dye reporter pairs for detecting YMOS sample solution, including β-CD·MB,[42] CB[6]·DSMI,[42] SC4A·OX1,[14] SC5A·LCG,[42] CAC4A·RhB, SAC5A·RhB,[43] and QAC5A·EY.[42] As presented in Fig. S1,† it suggested that the obvious modulated fluorescence intensity (I) was witnessed in CAC4A·RhB (1 μM/0.8 μM), SAC5A·RhB (1 μM/0.8 μM), and QAC5A·EY (0.4 μM/0.5 μM) reporter pairs in response to the addition of YMOS sample solution. The fluorescence intensity of the host·dye complex in HEPES buffer solution (10 mM, pH 7.4) was designated I_0. As shown in Fig. S1a–d,† there was no obvious modulation ($5 < |\Delta I(I - I_0)| < 65$) in fluorescence intensities of β-CD·MB, CB[6]·DSMI, SC4A·OX1, or SC5A·LCG in response to the YMOS sample solution (5 μL). It was noteworthy that CAC4A·RhB (1 μM/0.8 μM), SAC5A·RhB (1 μM/0.8 μM), and QAC5A·EY (0.4 μM/0.5 μM) reporter pairs enabled a significant "switch-on" fluorescence response ($128 \leq |\Delta I| \leq 538$) in the presence of YMOS sample solution (Fig. S1e–g†), which may be originated from deep cavitand of CAC4A, SAC5A, and QAC5A modified by azobenzene with negatively charged groups (carboxylated/sulfonated) or positively charged groups (quaternary ammonium). Therefore, we focused our attention on the three reporter pairs to construct the sensing array system for detection YMOS sample.

To ensure the feasibility and applicability of the established method, the precision, repeatability, and stability of the calixarene-based sensor array for sensing YMOS sample were further evaluated. In HEPES buffer solution, the YMOS sample solution (5 μL) was subjected to the detecting system of CAC4A·RhB (1 μM/0.8 μM), SAC5A·RhB (1 μM/0.8 μM), and QAC5A·EY (0.4 μM/0.5 μM), respectively. As illustrated in Fig. 1a, the RSD values for I/I_0 of the three sensing elements were less than 0.34%, indicating the good intra-day precision of the method. The repeated measurements (RSD < 5.74%) over consecutive three days confirmed the robust inter-day precision of the supramolecular fluorescence sensing method (Fig. 1b). The repeatability of this sensing array system was confirmed through the parallel preparation of six YMOS sample solutions, with an RSD of <5.54%, suggesting excellent repeatability, as depicted in Fig. 1c. Furthermore, the stability of the sensing array system over 10 consecutive hours has been demonstrated with an RSD of <4.37% (Fig. 1d). Generally, the methodological study indicated that the established supramolecular fluorescence sensor array was both reasonable and practicable for the quality evaluation of YMOS sample.

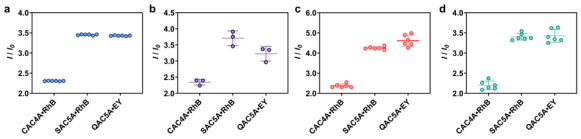

Fig. 1 The fluorescence response (I/I_0) for evaluating (a) intra-day precision ($n = 6$), (b) inter-day precision ($n = 3$), (c) repeatability ($n = 6$), and (d) stability ($n = 6$) of the supramolecular fluorescence sensing method.

Illustration on binding affinities between hosts and the tested compounds by fluorescence spectroscopy

The chemical basis of YMOS has been systematically reported in our previous work.[9] Based on UHPLC-Q-Orbitrap MS, we have thoroughly characterized the chemical composition of YMOS, successfully identifying a total of 67 compounds, which encompass flavonoids, nucleosides, terpene lactones, organic acids, additives, *etc.* Furthermore, 13 components were quantified by employing UPLC-PDA, revealing that QGR, Uri, Pra, and SoB (additive) were abundant in YMOS. Additionally, GinA is considered as the main active ingredient from GBE in YMOS.[44] Therefore, QGR, Uri, Pra, SoB, and GinA (Fig. S2†) were selected as the typical compounds to investigate their binding affinities with macrocyclic hosts.

Using the IDA strategy, we determined the K_a of the macrocycle·tested compound complex by employing fluorescence titration method.[45] GinA was taken as an example, as a representative insoluble compound.[46] As shown in Fig. S3a–c,† appropriate amount of methanol can improve solubility of GinA and had slight effect on the fluorescence intensity of CAC4A·RhB, SAC5A·RhB and QAC5A·EY reporter pairs. And, GinA had negligible effects on the fluorescence intensities of RhB and EY (Fig. S3d and e†). IDA execution validated the association constant ($K_a = (5.79 \pm 0.79) \times 10^6\ M^{-1}$) of CAC4A·RhB *via* fluorescence titration through 1 : 1 host–guest binding stoichiometry (Fig. S4†). The association constants of SAC5A·RhB ($K_a = (3.60 \pm 0.40) \times 10^6\ M^{-1}$) and QAC5A·EY ($K_a = (2.00 \pm 0.43) \times 10^7\ M^{-1}$) have been previously reported in the literature.[42,43] As depicted in Fig. 2, the gradual titration of GinA into the CAC4A·RhB (1.0 μM/0.8 μM), SAC5A·RhB (1.0 μM/0.8 μM), QAC5A·EY (0.4 μM/0.5 μM) reporter pairs resulted in the release of RhB/EY and a concomitant increase of fluorescent signals, respectively. In accordance with the competitive titration experiment, the association constants can be obtained as $K_{a(CAC4A\cdot GinA)} = (4.33 \pm 0.77) \times 10^4\ M^{-1}$, $K_{a(SAC4A\cdot GinA)} = (6.35 \pm 2.45) \times 10^5\ M^{-1}$, and $K_{a(QAC5A\cdot GinA)} = (5.50 \pm 1.52) \times 10^4\ M^{-1}$, respectively. Similarly, the association constants of QGR, SoB, Uri, and Pra with the three macrocycles were also determined (Fig. S5–S10†), respectively. The greater the value of the association constant is, the stronger the binding affinity between the macrocyclic host and the analyte is.[47] As shown in Table S1,† it is evident that the QAC5A had strong binding affinity to the five compounds and showed superior performance in sensing and detecting the main components from YMOS. The association affinities of QAC5A for the five analytes showed limited fluctuation, suggesting relatively low selectivity among the tested

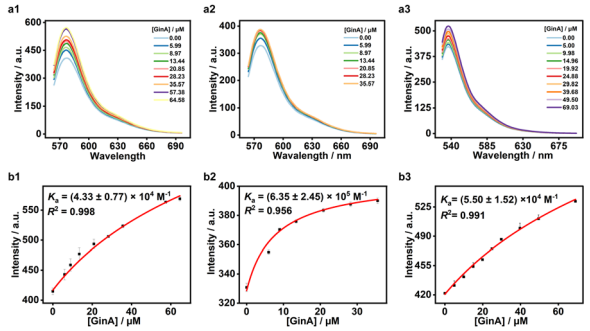

Fig. 2 Competitive fluorescence titration of CA·dye (CAC4A·RhB, SAC5A·RhB, and QAC5A·EY) reporter pairs with GinA in HEPES buffer solution (10 mM, pH 7.4) at 25 °C. (a1) Competitive titration in the CAC4A·RhB (1.0 μM/0.8 μM) reporter pair performed with GinA (up to 64.58 μM) at λ_{ex} = 554 nm. (b1) Competitive titration curve (λ_{em} = 576 nm) of the CAC4A·RhB (1.0 μM/0.8 μM) reporter pair with GinA acquired by a 1 : 1 competitive binding model (n = 3). (a2) Competitive titration in the SAC5A·RhB (1.0 μM/0.8 μM) reporter pair performed with GinA (up to 35.57 μM) at λ_{ex} = 554 nm. (b2) Competitive titration curve (λ_{em} = 576 nm) of SAC5A·RhB (1.0 μM/0.8 μM) reporter pair with GinA acquired by a 1 : 1 competitive binding model (n = 3). (a3) Competitive titration in the QAC5A·EY (0.4 μM/0.5 μM) reporter pair performed with GinA (up to 69.03 μM) at λ_{ex} = 517 nm. (b3) Competitive titration curve (λ_{em} = 537 nm) of QAC5A·EY (0.4 μM/0.5 μM) reporter pair with GinA acquired by a 1 : 1 competitive binding model (n = 3).

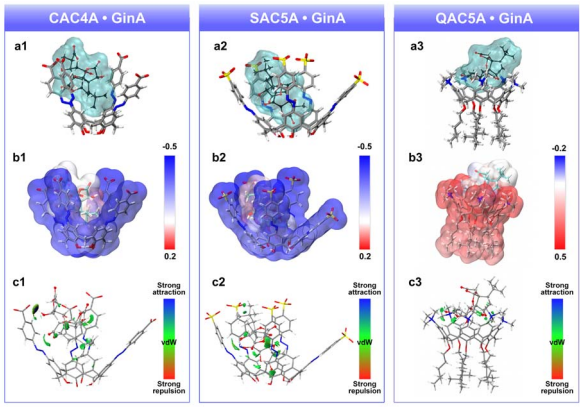

Fig. 3 Elucidation of the host·GinA complexes formation by theoretical calculations. (a1–a3) Optimized structures of the host·GinA complexes at B3LYP-D3(BJ)/6-31G (d)/SMD(water) level. (b1–b3) The molecular electrostatic potential (MEP, hartree) maps of the host·GinA complexes. (c1–c3) Noncovalent interactions in the host·GinA complexes by IGMH analysis. The isosurface (δ_g^{inter} = 0.005 a.u.) of the host·GinA complexes were colored with $(\lambda_2)\rho$ symbol.[35]

compounds. Nevertheless, CAC4A displayed both strong binding affinity and remarkable selectivity toward GinA. SAC5A exhibited differential binding behavior across SoB, GinA, and Uri, displaying strongest affinity to GinA. The observed differences can be attributed to cavity dimensions, spatial arrangement of functional groups, and framework rigidity. The association constants of CAC4A·QGR, CAC4A·SoB, CAC4A·Uri, CAC4A·Pra, SAC5A·QGR, and SAC5A·Pra were not detected, which could be attributed to the inappropriate non-covalent interaction between the hosts and the guests.

Investigation on intermolecular interactions between hosts and the tested compounds by theoretical calculation and NMR

Density functional theory (DFT) is a computational modeling method grounded in quantum mechanics, which can be utilized to investigate the geometric structure and energy properties of molecules. It is frequently employed to explore microscopic mechanisms at the molecular and electronic levels, thereby facilitating the comprehension and visualisation of molecular configurations.[48] It serves as a powerful method for assessing the interaction mechanism between host and guest in supramolecular chemistry.[49,50] In response to this point, theoretical simulations of the geometric structures of host·analyte complexes with binding affinity were performed in this study using DFT at the B3LYP-D3(BJ)/6-31G(d)/SMD(water). The host·GinA complex was used as an example to illustrate the non-covalent interactions between the host and the analyte. As shown in Table S2,† the binding energies (ΔE) of the host·analyte complexes were negative, confirming that the inclusion of the GinA within the hosts cavity were thermodynamically stable, respectively. Fig. 3a1–a3 illustrates the results of structural optimization for GinA in conjunction with the three hosts based on DFT, demonstrating the formation of inclusion complexes between each host and GinA.

The molecular electrostatic potential (MEP) analysis elucidates interactions between molecules and other molecules by calculating the electron number and charge distribution within a molecular structural model, and it can identify potential binding sites for intermolecular reactions.[20,28] To obtain deeper insights into the host·guest interactions, the MEP were computed and mapped on the van der Waal (vdW) surfaces of hosts and GinA. As depicted in Fig. 3b1 and b2, CAC4A and SAC5A are electron-rich, particularly at the upper rim, which are modified by azobenzene moieties with negatively charged groups (carboxylated/sulfonated). The QAC5A molecule exhibited electron deficiency, especially notable in the region proximal to the upper rim decoration of the quaternary ammonium groups (Fig. 3b3). The GinA molecule boasts *tert*-butyl, hydroxyl, and carbonyl substituents, which is propitious to the optimized geometry of host·GinA complexes because molecules are always prone to interact with each other in a MEP-complementary manner.

The independent gradient model (IGMH) analysis is mainly used to elucidate the weak interactions that exist between molecules.[35] In order to provide a more distinct description of the non-covalent binding forms between the host and GinA, the rings in GinA were labeled (Fig. S2†). By the IGMH analysis, –COOH in CAC4A formed a strong hydrogen bond O–H···O with the –OH of E-ring in GinA (the blue isosurfaces). The green isosurfaces in the IGMH analysis further revealed many weak interactions between CAC4A and GinA, including the C–H···O (–CH_3 of E-ring in GinA and –COOH in CAC4A), Ar–H···O (Ar–H in CAC4A and –C=O of D-ring in GinA), C–H···N (*tert*-butyl in

GinA and azo group in CAC4A), O–H···π (–OH of C-ring in GinA and Ar–H in CAC4A), C–H···π (*tert*-butyl in GinA and benzene ring in CAC4A), and vdw interactions (Fig. 3c1 and S11a†). The azo group of SAC5A formed a strong hydrogen bond (O–H···N) with the hydroxyl group in C-ring in GinA (the blue isosurfaces). Moreover, the green isosurfaces in the IMGH analysis further uncovered many weak interactions between SAC5A and GinA, including the C–H···O (*tert*-butyl in GinA and –SO_3H in SAC5A), Ar–H···O (Ar–H in SAC5A and –C═O of C-ring in GinA), O–H···π (–OH of E-ring in GinA and benzene ring in SAC5A), C–H···π (C–H in B-ring in GinA and benzene ring in SAC5A), and vdw interactions (Fig. 3c2 and S11b†). For the complex of QAC5A·GinA, the –C═O and –O– in E-ring and D-ring of GinA were witnessed to be hydrogen bond acceptors, while C–H from quaternary amino group in QAC5A can be hydrogen bond donors (Fig. 3c3 and S11c†). It can also be concluded that the benzene ring in QAC5A is played as hydrogen bond acceptors, while C–H of B-ring in GinA could be hydrogen bond donors. Generally, the underlying various non-covalent interactions between calixarenes and GinA, including hydrogen bonding, electrostatic interaction, and hydrophobic interaction. The macrocyclic compound SAC5A was selected for ^{1}H NMR characterization of its complex with GinA in D_2O based on its excellent water solubility, whose result was shown in Fig. S12.† Upon the formation of an inclusion complex, characteristic upfield shifts ($\Delta\delta$ = 0.04–0.20 ppm) of GinA protons were witnessed by NMR analysis, arising from SAC5A's aromatic ring current.

Shortly, different macrocycles exhibit distinct binding affinities for the same analyte in terms of non-covalent interactions. Different analytes may also have the same non-covalent interactions with the focused macrocycle. For instance, the hydroxyl group of Uri formed a strong hydrogen bond (O–H···N) with the azo group of SAC5A (Fig. S13a†), which was similar to the case of SAC5A·GinA. Moreover, in the non-covalent interactions between QAC5A and Uri, the binding affinity was stronger according to K_a (Table S1†), characterized by N–H···π, C–H···O, and C–H···π interactions (Fig. S13b†). In general, the intermolecular binding behaviors are closely related to the molecular structures. The non-covalent interactions between hosts and analysts were listed detailedly in Table S3.†

Evaluation of YMOS sample quality consistency and precise control of feeding by using the calixarene-based sensor array

Twelve batches of YMOS samples (YM1–YM12) were analyzed using the established calixarene-based sensor array. As illustrated in Fig. 4a–c, the fluorescent fingerprints were generated by analyzing the responses (switch-on) of the CAC4A·RhB (1.0 μM/0.8 μM), SAC5A·RhB (1.0 μM/0.8 μM), and QAC5A·EY (0.4 μM/0.5 μM) reporter pairs upon exposure to the YMOS sample solution (5 μL) in HEPES buffer solution, respectively. The fluorescence intensities of the respective reporter pairs were recorded before (I_0) and after (I) the addition of the YMOS sample solution. The average values of I/I_0 for the respective reporter pairs exhibited robust consistency among the tested

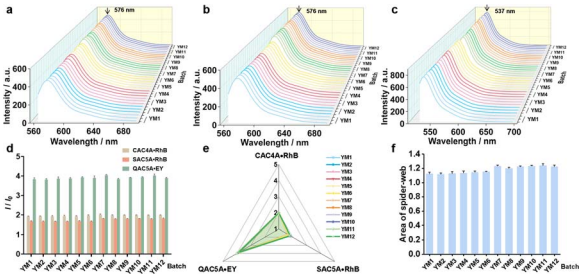

Fig. 4 The fluorescence emission spectra of CAC4A·RhB (a), SAC5A·RhB (b), QAC5A·EY (c) reporter pairs for 12 batches of qualified YMOS samples (n = 3). (d) The fluorescence fingerprint of the three sensing elements for 12 batches of qualified YMOS samples (n = 3). The "spider-web" diagram (e) and area of "spider-web" (f) for 12 batches of YMOS samples.

batches of YMOS, as depicted in Fig. 4d. To visually illustrate the response of the sensing elements to multiple batches of YMOS samples, the "spider-web" mode was employed, offering a comprehensive assessment of YMOS quality.[51,52] Specifically, the I/I_0 values measured by each sensing element were denoted as A_{m-k} and correspondingly divided by the maximum I/I_0 of the focused sensing element ($A_{m(\max)}$) to obtain E_{m-k} (Table S4†). In eqn (1), m represents different sensing elements, and k represents different batches. E_{m-k} values were used to define different dimensions (p_i) in eqn (2), with the angle between any two dimensions labeled as α ($\alpha = 360°/n$, n = 3), respectively. Eqn (2) was further utilized to calculate the shadowed area of the "spider-web" mode. Fig. 4e, f and Table S5† demonstrated that the shadow areas in the "spider-web" pattern are consistent across six batches of YMOS.

$$E_{m-k} = A_{m-k}/A_{m(\max)} \quad (1)$$

$$S = \frac{1}{2}\sin\alpha\left(\sum_{i=1}^{n-1} p_i \times p_{i+1} + p_n \times p_1\right) \quad (2)$$

In order to further investigate the application of the quality evaluation method of YMOS based on calixarene-based sensor array strategy in TCM production processes, the QAC5A·EY complex was employed to guarantee the precise feeding of GBE and AME for production of YMOS. As illustrated in Fig. 5, different combinations of GBE and AME (GBE : AME = 0 : 30, 1 : 30, 3 : 30, 6 : 30; g g^{-1}) were prepared to obtain self-made YMOS sample solutions. The fluorescence intensity of the QAC5A·EY (0.4 μM/0.5 μM) complex was recorded before and after adding 5 μL self-made YMOS sample solution, labeled as I_0 and I, respectively. And, the fluorescence response was evaluated with I/I_0 (Table S6†), which was statistically significant across different combinations of GBE and AME (***p < 0.001). Therefore, the QAC5A·EY reporter pair based on supramolecular fluorescence sensing strategy is capable of monitoring the dosage of Chinese medicinal materials in preparations, which can be effectively applied to the evaluation of the preparation process on production lines. The analytical results obtained from the aforementioned actual samples demonstrate that the

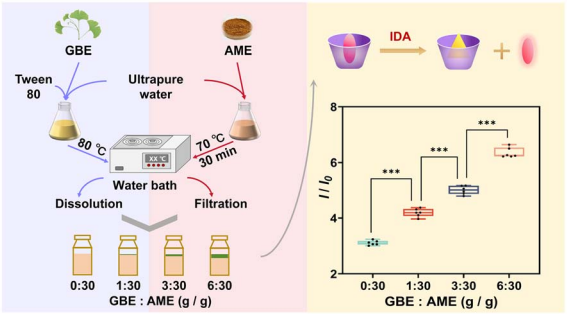

Fig. 5 The process steps of self-made YMOS samples and the fluorescence response of QAC5A·EY (0.4 μM/0.5 μM) complex to self-made YMOS samples ($n = 3$, ***$p < 0.001$).

calixarene-based fluorescence sensing method is feasible for application in the quality assessment of TCM. A comprehensive comparison with other sensing techniques is systematically elaborated in Table S7.†

Conclusions

In this study, a facile calixarene-based sensor array method was constructed for assessing quality consistency of YMOS, which was proved to be feasible and high efficient. Based on the IDA strategy, the calixarenes formed complexes with components in YMOS by their intermolecular interactions, leading to modulations in the fluorescence signal of the sensing system. The established method has been successfully applied to evaluate the inter-batch consistency and monitor the feeding ratio of GBE and AME in production of YMOS. Herein, we aim to provide new methods for the quality consistency evaluation and formulation process monitoring of YMOS and other TCM preparations.

Data availability

The data supporting this article have been included as part of the ESI.†

Author contributions

K. Niu: writing – original draft, software, methodology, M. Ye: conceptualization, methodology. Y. Lyu: data curation, validation. W. Cheng: visualization, data curation. S. He: supervision. D. Liu: conceptualization, supervision. H. Yu: supervision, foundation, writing – original draft, writing – review & editing.

Conflicts of interest

There are no conflicts to declare.

Acknowledgements

This work was supported by the Science and Technology Program of Tianjin in China (24ZYJDSS00300), National Natural Science Foundation of China (82204769), Special Project for Technological Innovation in New Productive Forces of Modern Chinese Medicines (24ZXZKSY00010), and Development of a Chemical Information Knowledgebase for Warming and Qi-Regulating Herbs.

References

1 X. Chen, C. Yang, H. Chen, L. Sun, L. Liu, C. Wu and L. Wang, Research of preparation process of Chinese materia medica compound preparation based on characteristics of Chinese materia medica compound preparation, *Zhongcaoyao*, 2021, **52**, 5807–5813.
2 M. He, S. Mao, Q. Du, X. Gao, J. Shi, X. Zhou, F. Zhang, Y. Lu, H. Wang, Y. Yu, L. Sun and X. Zhang, Integration of fingerprint-activity relationship and chemometric analysis to accurately screen Q-markers for the quality control of traditional Chinese medicine compound preparation: Jinlian Qingre granules as an example, *Arab. J. Chem.*, 2024, **17**, 105481.
3 X. C. Wei, B. Cao, C. H. Luo, H. Z. Huang, P. Tan, X. R. Xu, R. C. Xu, M. Yang, Y. Zhang, L. Han and D. K. Zhang, Recent advances of novel technologies for quality consistency assessment of natural herbal medicines and preparations, *Chin. Med.*, 2020, **15**, 56.
4 A. Zhao, L. Xiao, S. Chen, H. Yi, J. Di, C. Guo, J. Cheng, J. Zhang, J. Jiang, J. Zhang, Y. Liu and A. Liu, Comprehensive quality consistency evaluation strategy and analysis of compound danshen tablet, *J. Pharm. Biomed. Anal.*, 2022, **219**, 114951.
5 M. J. Yao, X. D. Fan, B. Yang, L. Xu, W. T. Song, G. R. Wang, X. X. Dong and J. X. Liu, Ginkgo leaf extract and Armillaria mellea powders oral attenuates inflammation of microglia in habenular nucleus through CX3CL1-CX3CR1 axis in post stroke depression, *Chin. J. Pharmacol. Toxicol.*, 2019, **33**, 700–701.
6 Chinese Pharmacopoeia Commission, *Pharmacopoeia of the People's Republic of China*, Chinese Medical Science and Technology Press, Beijing, 2020.
7 L. Wang, *China Pat.*, CN 103364520 A, 2013.
8 C. Liu, *MD Master Thesis*, Chengdu University, 2021.
9 G. Xue, N. Meng, Y. Zhao, R. Zhang, J. Yang, Z. Chen, M. Zhang and X. Chai, The qualitative and quantitative profiling for quality assessment of Yinxing Mihuan oral solution and the stability study on the focused flavonol glycosides, *J. Pharm. Biomed. Anal.*, 2022, **219**, 114937.
10 Y. Jin, J. Pan and K. Cheng, Quality assessment of compound Yuxingcao mixture produced by different manufacturers using high performance liquid chromatography and near infrared spectroscopy combined with multivariate algorithms, *Infrared Phys. Technol.*, 2024, **139**, 105337.
11 Q. Chang, L. Lan, D. Gong, Y. Guo and G. Sun, Evaluation of quality consistency of herbal preparations using five-wavelength fusion HPLC fingerprint combined with ATR-FT-IR spectral quantized fingerprint: Belamcandae rhizoma antiviral injection as an example, *J. Pharm. Biomed. Anal.*, 2022, **214**, 114733.

12 J. H. Tian, Y. L. Lin, J. J. Li, R. Ma, H. Yu, Y. Wang, X. Y. Hu and D. S. Guo, Supramolecular fluorescence sensing for quality evaluation of traditional Chinese medicine, *Arab. J. Chem.*, 2023, **16**, 104974.
13 C. Guo, A. C. Sedgwick, T. Hirao and J. L. Sessler, Supramolecular Fluorescent Sensors: An Historical Overview and Update, *Coord. Chem. Rev.*, 2021, **427**, 213560.
14 H. Yu, X. Chai, W. C. Geng, L. Zhang, F. Ding, D. S. Guo and Y. Wang, Facile and label-free fluorescence strategy for evaluating the influence of bioactive ingredients on FMO3 activity via supramolecular host-guest reporter pair, *Biosens. Bioelectron.*, 2021, **192**, 113488.
15 M. Li, H. Yu, Y. Li, X. Li, S. Huang, X. Liu, G. Weng, L. Xu, T. Hou, D.-S. Guo and Y. Wang, Rational design of supramolecular self-assembly sensor for living cell imaging of HDAC1 and its application in high-throughput screening, *Biosens. Bioelectron.*, 2023, **242**, 115716.
16 D. Wang, W. Li, W. Cheng, Y. Wang, Z. Zheng, X. Y. Hu, H. Y. Wang, X. Zhang, H. Yu, D. S. Guo and Y. Wang, Guest adaptative supramolecular sensing strategy for warning the risky aflatoxins in contaminated cereals, *J. Hazard. Mater.*, 2024, **464**, 133015.
17 L. You, D. Zha and E. V. Anslyn, Recent Advances in Supramolecular Analytical Chemistry Using Optical Sensing, *Chem. Rev.*, 2015, **115**, 7840–7892.
18 T. Li, X. Zhu, X. Hai, S. Bi and X. Zhang, Recent Progress in Sensor Arrays: From Construction Principles of Sensing Elements to Applications, *ACS Sens.*, 2023, **8**, 994–1016.
19 K. J. Albert, N. S. Lewis, C. L. Schauer, G. A. Sotzing, S. E. Stitzel, T. P. Vaid and D. R. Walt, Cross-Reactive Chemical Sensor Arrays, *Chem. Rev.*, 2000, **100**, 2595–2626.
20 W. Geng, Z. Zheng, H. Jiang and D. Guo, Nucleotide Recognition by a Guanidinocalixarene Receptor in Aqueous Solution, *Chem. Res. Chin. Univ.*, 2023, **39**, 144–150.
21 Z. Zheng, W. C. Geng, J. Gao, Y. J. Mu and D. S. Guo, Differential calixarene receptors create patterns that discriminate glycosaminoglycans, *Org. Chem. Front.*, 2018, **5**, 2685–2691.
22 J. H. Tian, X. Y. Hu, Z. Y. Hu, H. W. Tian, J. J. Li, Y. C. Pan, H. B. Li and D. S. Guo, A facile way to construct sensor array library via supramolecular chemistry for discriminating complex systems, *Nat. Commun.*, 2022, **13**, 4293.
23 S. Shinkai, S. Mori, T. Tsubaki, T. Sone and O. Manabe, New water-soluble host molecules derived from calix[6]arene, *Tetrahedron Lett.*, 1984, **25**, 5315–5318.
24 J. W. Steed, C. P. Johnson, C. L. Barnes, R. K. Juneja, J. L. Atwood, S. D. Reilly, R. L. Hollis, P. Smith and D. L. Clark, Supramolecular Chemistry of *p*-Sulfonatocalix[5]arene: A Water-Soluble, Bowl-Shaped Host with a Large Molecular Cavity, *J. Am. Chem. Soc.*, 1995, **117**, 11426–11433.
25 S. Shinkai, S. Mori, H. Koreishi, T. Tsubaki and O. Manabe, Hexasulfonated calix[6]arene derivatives: a new class of catalysts, surfactants, and host molecules, *J. Am. Chem. Soc.*, 1986, **108**, 2409–2416.
26 J. S. Guo, J. J. Li, Z. H. Wang, Y. Liu, Y. X. Yue, H. B. Li, X. H. Zhao, Y. J. Sun, Y. H. Ding, F. Ding, D. S. Guo, L. Wang and Y. Chen, Dual hypoxia-responsive supramolecular complex for cancer target therapy, *Nat. Commun.*, 2023, **14**, 5634.
27 W. C. Geng, S. Jia, Z. Zheng, Z. Li, D. Ding and D. S. Guo, A Noncovalent Fluorescence Turn-on Strategy for Hypoxia Imaging, *Angew. Chem., Int. Ed.*, 2019, **58**, 2377–2381.
28 W. Li, H. Dong, K. Niu, H. Y. Wang, W. Cheng, H. Song, A. K. Ying, X. Zhai, K. Li, H. Yu, D. S. Guo and Y. Wang, Analyzing urinary hippuric acid as a metabolic health biomarker through a supramolecular architecture, *Talanta*, 2024, **278**, 126480.
29 X. You, *China Pat.*, CN 1899324A, 2007.
30 H. Yu, W. C. Geng, Z. Zheng, J. Gao, D. S. Guo and Y. Wang, Facile Fluorescence Monitoring of Gut Microbial Metabolite Trimethylamine *N*-oxide via Molecular Recognition of Guanidinium-Modified Calixarene, *Theranostics*, 2019, **9**, 4624–4632.
31 M. J. Frisch, G. W. Trucks, H. B. Schlegel, G. E. Scuseria, M. A. Robb, J. R. Cheeseman, G. Scalmani, V. Barone, G. A. Petersson, H. Nakatsuji, X. Li, M. Caricato, A. V. Marenich, J. Bloino, B. G. Janesko, R. Gomperts, B. Mennucci, H. P. Hratchian, J. V. Ortiz, A. F. Izmaylov, J. L. Sonnenberg, D. Williams-Young, F. Ding, F. Lipparini, F. Egidi, J. Goings, B. Peng, A. Petrone, T. Henderson, D. Ranasinghe, V. G. Zakrzewski, J. Gao, N. Rega, G. Zheng, W. Liang, M. Hada, M. Ehara, K. Toyota, R. Fukuda, J. Hasegawa, M. Ishida, T. Nakajima, Y. Honda, O. Kitao, H. Nakai, T. Vreven, K. Throssell, J. A. Montgomery Jr, J. E. Peralta, F. Ogliaro, M. J. Bearpark, J. J. Heyd, E. N. Brothers, K. N. Kudin, V. N. Staroverov, T. A. Keith, R. Kobayashi, J. Normand, K. Raghavachari, A. P. Rendell, J. C. Burant, S. S. Iyengar, J. Tomasi, M. Cossi, J. M. Millam, M. Klene, C. Adamo, R. Cammi, J. W. Ochterski, R. L. Martin, K. Morokuma, O. Farkas, J. B. Foresman and D. J. Fox, *Gaussian 16 Revision C.01*, 2016.
32 A. V. Marenich, C. J. Cramer and D. G. Truhlar, Universal solvation model based on solute electron density and on a continuum model of the solvent defined by the bulk dielectric constant and atomic surface tensions, *J. Phys. Chem. B*, 2009, **113**, 6378–6396.
33 P. J. Stephens, F. J. Devlin, C. F. Chabalowski and M. J. Frisch, Ab Initio Calculation of Vibrational Absorption and Circular Dichroism Spectra Using Density Functional Force Fields, *J. Phys. Chem.*, 1994, **98**, 11623–11627.
34 S. Grimme, J. Antony, S. Ehrlich and H. Krieg, A consistent and accurate ab initio parametrization of density functional dispersion correction (DFT-D) for the 94 elements H-Pu, *J. Chem. Phys.*, 2010, **132**, 154104.
35 T. Lu and Q. Chen, Independent gradient model based on Hirshfeld partition: A new method for visual study of interactions in chemical systems, *J. Comput. Chem.*, 2022, **43**, 539–555.
36 W. Humphrey, A. Dalke and K. Schulten, VMD: visual molecular dynamics, *J. Mol. Graph.*, 1996, **14**, 33–38.

37 T. L. Mako, J. M. Racicot and M. Levine, Supramolecular Luminescent Sensors, *Chem. Rev.*, 2018, **119**, 322–477.
38 A. C. Sedgwick, J. T. Brewster, T. Wu, X. Feng, S. D. Bull, X. Qian, J. L. Sessler, T. D. James, E. V. Anslyn and X. Sun, Indicator displacement assays (IDAs): the past, present and future, *Chem. Soc. Rev.*, 2021, **50**, 9–38.
39 G. Crini, Review: A History of Cyclodextrins, *Chem. Rev.*, 2014, **114**, 10940–10975.
40 R. Kumar, A. Sharma, H. Singh, P. Suating, H. S. Kim, K. Sunwoo, I. Shim, B. C. Gibb and J. S. Kim, Revisiting Fluorescent Calixarenes: From Molecular Sensors to Smart Materials, *Chem. Rev.*, 2019, **119**, 9657–9721.
41 K. Kim, N. Selvapalam, Y. H. Ko, K. M. Park, D. Kim and J. Kim, Functionalized cucurbiturils and their applications, *Chem. Soc. Rev.*, 2007, **36**, 267–279.
42 Y. Zhang, H. Yu, S. Chai, X. Chai, L. Wang, W. C. Geng, J. J. Li, Y. X. Yue, D. S. Guo and Y. Wang, Noninvasive and Individual-Centered Monitoring of Uric Acid for Precaution of Hyperuricemia via Optical Supramolecular Sensing, *Adv. Sci.*, 2022, **9**, e2104463.
43 Y. X. Yue, Y. L. Lin, M. M. Chen, H. W. Tian, R. Ma, Z. H. Wang, F. Y. Chen, Y. C. Pan and D. S. Guo, Azocalixarenes: a scaffold of universal excipients with high efficiency, *Sci. China Chem.*, 2024, **67**, 1697–1706.
44 H. Kuribara, S. T. Weintraub, T. Yoshihama and Y. Maruyama, An anxiolytic-like effect of Ginkgo biloba extract and its constituent, ginkgolide-A, in mice, *J. Nat. Prod.*, 2003, **66**, 1333–1337.
45 Y. X. Yue, Y. Kong, F. Yang, Z. Zheng, X. Y. Hu and D. S. Guo, Supramolecular Tandem Assay for Pyridoxal-5′-phosphate by the Reporter Pair of Guanidinocalix[5]Arene and Fluorescein, *ChemistryOpen*, 2019, **8**, 1437–1440.
46 T. Q. Rui, L. Zhang, H. Z. Qiao, P. Huang, S. Qian, J. S. Li, Z. P. Chen, T. M. Fu, L. Q. Di and B. Cai, Preparation and Physicochemical and Pharmacokinetic Characterization of Ginkgo Lactone Nanosuspensions for Antiplatelet Aggregation, *J. Pharm. Sci.*, 2016, **105**, 242–249.
47 K. N. Houk, A. G. Leach, S. P. Kim and X. Zhang, Binding Affinities of Host–Guest, Protein–Ligand, and Protein–Transition-State Complexes, *Angew. Chem., Int. Ed.*, 2003, **42**, 4872–4897.
48 X. Wu, M. V. Cañamares, I. Kakoulli and S. Sanchez-Cortes, Chemical Characterization and Molecular Dynamics Simulations of Bufotenine by Surface-Enhanced Raman Scattering (SERS) and Density Functional Theory (DFT), *J. Phys. Chem. Lett.*, 2022, **13**, 5831–5837.
49 C. Shen, Z. Gong, L. Gao, M. Gu, L. Huan, S. Wang and J. Xie, Theoretical study on host-guest interaction between pillar[4] arene and molecules or ions, *J. Mol. Model.*, 2018, **24**, 199.
50 J. Xie, Z. Xi, Z. Yang, X. Zhang, H. Yuan, Y. Yang, L. Ni and M. He, Computational approach to understanding the structures, properties, and supramolecular chemistry of pagoda[n]arenes, *J. Mol. Struct.*, 2023, **1281**, 135073.
51 D. N. Wang, J. M. Ding, X. Chai, J. Yang and Y. F. Wang, Application of “spider-web” mode in research of Chinese materia medica, *Zhongcaoyao*, 2019, **50**, 4582–4588.
52 Z. Z. Jiang, J. Yang and Y. F. Wang, Discrimination and identification of Q-markers based on 'Spider-web' mode for quality control of traditional Chinese medicine, *Phytomedicine*, 2018, **44**, 98–102.